PACS numbers: 42.55.Px; 42.60.Jf
DOI: 10.1070/QE2000v030n05ABEH001732

Brightness and filamentation of a beam from powerful cw quantum-well $In_{0.2}Ga_{0.8}As/GaAs$ lasers

A P Bogatov, A E Drakin, A A Stratonnikov, V P Konyaev

Abstract. Near- and far-field patterns are studied for powerful (above 2-W cw output) quantum-well heterojunction InGaAs/AlGaAs/GaAs lasers. The maximum radiation brightness was $1.7 \cdot 10^7$ W cm^{-2} sr^{-1}. It is shown that the radiation filamentation is already observed 10 – 20% above the lasing threshold. The filamentation period decreases from 50 to 10 μm with increasing pumping current from almost the lasing threshold to an excess of 20% over the threshold. The filamentation results in the tenfold decrease in the radiation brightness of lasers compared to the theoretical value.

1. Introduction

Presently, semiconductor lasers with a power above 1 W are attracting great interest because they are desirable for many applications. In this respect, among the most promising are powerful InGaAs/GaAs heterojunction lasers, an important parameter of whose is beam divergence. In early studies of AlGaAs heterojunction lasers, it has been shown that this parameter can substantially exceed the diffraction limit. This is mainly explained by the appearance of the transverse instability of the optical flux [1 – 5], which results in the transverse periodical spatial modulation of its intensity or, in other words, in the appearance of filamentation [6].

By now, it has been found [3 – 5] that filamentation is caused by optical nonlinearity due to the dependence of the refractive index of a semiconductor on the concentration of nonequilibrium charge carriers. To suppress the transverse instability, several designs of powerful semiconductor lasers have been devised and implemented (see, for example, [7 – 9]). The filamentation threshold in these lasers was increased to achieve the 1-W output with the beam divergence being close to the diffraction limit in both transverse directions.

The filamentation threshold and behaviour of filaments depend on the parameters of a medium that characterise optical nonlinearity, in particular, on its energy level diagram and the waveguide construction of the laser. For this reason, each new design of a semiconductor laser requires a special study of the filament structure with the aim of finding the filamentation threshold and determining the characteristic trans-verse spatial instability harmonics that possess the maximum instability increment. The properties of these harmonics can be used to suppress filamentation, thereby increasing the brightness of laser radiation.

The goal of this paper is to study filamentation in powerful (above 2-W cw output) quantum-well InGaAs/GaAs lasers operating at room temperature without forced cooling.

2. Experimental

We paid most of our attention to the study of near- and far-field patterns of experimental samples in the horizontal yz plane (Fig. 1), because it is the direction Oy lying in the $p - n$ transition plane that is of primary interest. The resonator width in this direction is 100 μm; i.e., it is two orders of magnitude greater than the radiation wavelength, and the resonator has a great number of allowed transverse modes in this direction with close quality factors. In addition, in this direction, the nonlinear self-deformation of the transverse distribution of the optical flux takes place, which results in filamentation. For this reason, the resulting transverse intensity distribution and the radiation pattern in the Oy direction yield information on the characteristic period of the filamentation pattern and the beam divergence in the far field, and also allow one to measure the radiation brightness — a parameter that is important for practical applications.

In a classical sense, the brightness is a light flux emitted into the unit solid angle by the unit area of the emitting surface

$$B = P/S\Omega, \tag{1}$$

where P is the radiation power; S is the emitting surface; and Ω is the solid angle into which the power P is emitted. For the divergence that is close to the diffraction one, such a definition becomes approximate, and in our case, it is

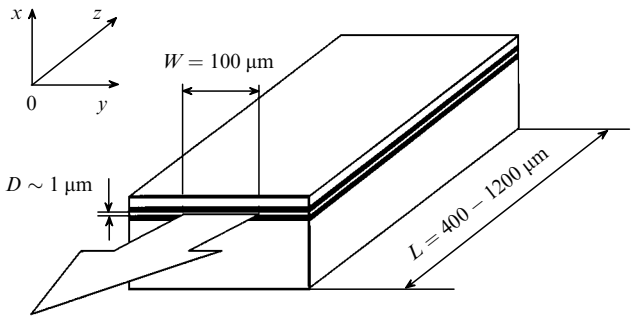

Figure 1. Schematic of a laser (D is the effective transverse size filled by an optical flux).

A P Bogatov, A E Drakin, A A Stratonnikov, V P Konyaev P N Lebedev Physics Institute, Russian Academy of Sciences, Leninskii prosp. 53, 117924 Moscow, Russia

Received 29 December 1999
Kvantovaya Elektronika **30** (5) 401 – 405 (2000)
Translated by M N Sapozhnikov

convenient to represent Eqn (1) in the form

$$B = P\frac{1}{D_x\varphi_x}\frac{1}{D_y\varphi_y}, \tag{2}$$

where D_x and D_y are sizes of the emitting surface; φ_x and φ_y are angular divergences of radiation in planes xz and yz, respectively (Fig. 1).

We will show below that the laser under study emits at a single (zero) mode in the Ox direction. If D_x and φ_x are defined as

$$D_x = 0.64\frac{\int I(x)\mathrm{d}x}{I_{\max}(x)}, \qquad \varphi_x = 0.64\frac{\int I(\varphi)\mathrm{d}\varphi}{I_{\max}(\varphi)}, \tag{3}$$

where $I(x)$ and $I(\varphi)$ are the spatial and angular dependences of radiation in the near and far fields; $I_{\max}(x)$ and $I_{\max}(\varphi)$ are their maximum values; and the numerical coefficient 0.64 corresponds to specific distributions $I(x)$ and $I(\varphi)$ for the structures whose parameters are presented in Table 1, then we should substitute the expression

$$D_x\varphi_x = \lambda, \tag{4}$$

(where λ is the radiation wavelength in air) into (2).

In the Oy direction, lasing occurs at several modes. Because we can only observe the field intensity rather than its amplitude, we do not know exactly the energy distribution over the modes. For this reason, here we use a classical approach in describing the brightness. The size D_y of the emitting surface was assumed equal to the width of the pumping region because the active region emits the radiation over its whole width. The angular divergence φ_y was determined from the far-field pattern $I(\varphi)$ as

$$\varphi_y = \frac{\int I(\varphi)\mathrm{d}\varphi}{I_{\max}(\varphi)}. \tag{5}$$

Fig. 2 shows the schematic of the setup for measuring the radiation pattern of lasers. Sample *4* was placed on turning table *5*, which was rotated in the horizontal plane with a computer-controlled step motor *10*. The laser radiation was incident on vertical slit *6* and was focussed with lens *7* (in the vertical direction) on a measuring photodiode *8* operating in the photodiode mode. The output signal was fed via ADC *9* to a computer.

This system scanned the radiation pattern by rotating the turning table with the sample. The initial position of the table was determined by using the reference system that consisted of reference laser *1*, totally reflecting mirror *3*, and reference detector (photodiode) *2*. This system provided the angular

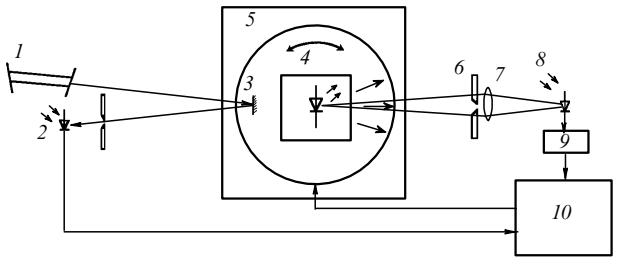

Figure 2. Schematic of the setup for measuring the radiation pattern of lasers.

resolution of the radiation pattern about of 0.5°, with the referencing to the zero angle relative to the normal to the laser diode face being no worse than 1.5° and the referencing drift being no worse than 0.1°.

The near-field pattern of laser diodes was studied using an optical multichannel analyser. The image of the output mirror of the sample was projected on the photosensitive surface of the analyser. The image was magnified approximately by a factor of 70 using a microlens, the surface of the laser diode being in the focus of the microlens. This optical system had a resolution of ~ 3 μm.

The light output – current characteristics of samples were measured in a calibrated photometric sphere, inside which a laser and germanium photodiode were placed.

We studied samples grown on the basis of the GaAs/AlGaAs/InGaAs structures of three types (Table 1). Layers 4 and 6 are active, the core of a waveguide is formed in the vertical direction by layers 2 and 8, and layers 1 and 9 serve as the waveguide cladding.

The width of a strip contact for the current injection was 100 μm. One resonator mirror was covered with an antireflection coating (the reflection coefficient was $R = 12\%$) and the other one was highly reflecting ($R = 97\%$), so that radiation emerged only from one side of the laser. Samples were soldered on a bulky metal body to provide the efficient heat removal for pump currents up to 2.5 A without forced cooling. The lasers under study emitted near 1050 nm.

Fig. 3 shows experimental and theoretical far-field patterns in the vertical plane for sample No. 1. The experimental pattern was obtained for the pump current equal to 2 A, and the theoretical pattern was calculated for the zero mode for the parameters of this sample presented in Table 1. Because the composition of the grown structure does not exactly coincide with the composition that has been designed, we made a correction of the refractive index

Table 1. Structures of laser diodes studied.

Layer number	Composition	Refractive index	Sample thickness (μm)		
			Sample No. 1	Sample No. 2	Sample No. 3
1	$Al_{0.30}Ga_{0.70}As$	3.340	4.8	2.8	3.0
2	$Al_{0.26}Ga_{0.74}As$	3.365	1.0	0.2	0.3
3	GaAs	3.52	0.0070	0.0070	0.0070
4	$In_{0.20}Ga_{0.80}As$	3.60	0.0053	0.0053	0.0053
5	GaAs	3.52	0.0100	0.0100	0.0070
6	$In_{0.20}Ga_{0.80}As$	3.60	0.0053	0.0053	0.0053
7	GaAs	3.52	0.0070	0.0070	0.0070
8	$Al_{0.26}Ga_{0.74}As$	3.365	1.0	0.2	0.3
9	$Al_{0.30}Ga_{0.70}As$	3.340	1.6	1.9	1.5
10	GaAs	3.52		Substrate	

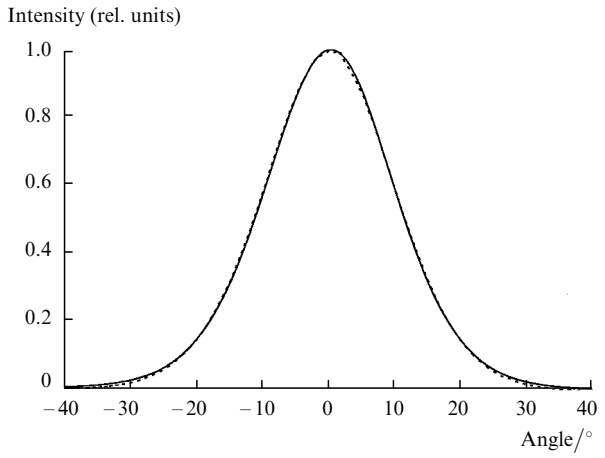

Figure 3. Calculate (soid curve) and experimental (dashed curve) far-field patterns in the vertical direction (the xz plane) for sample No. 1 for the pump current equal to 2 A.

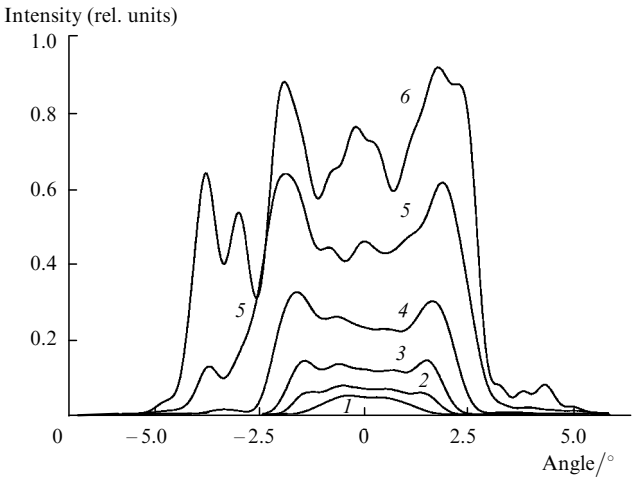

Figure 5. Far-field patterns for sample No. 1 in the horizontal direction (the yz plane) for pump currents 285 (1), 310 (2), 350 (3), 450 (4), 700 (5), and 1000 mA (6).

of the waveguide layers to obtain the coincidence between the calculated and experimental far-field divergence. The result obtained shows that, first, in the vertical direction, lasing occurs only at a single (zero) mode and, second, Eqn (4) can be used, in which the numerical coefficient 0.64 was found taking into account specific intensity distribution functions $I(x)$ and $I(\varphi)$ in the near and far zones.

The emission spectra of lasers under study were detected by focusing a laser beam on the entrance slit of a monochromator equipped with an optical multichannel analyser placed instead of its exit slit. The image of the spectrum formed in the exit-slit plane was detected with an optical multichannel analyser.

3. Results of measurements and discussion

Fig. 4 shows light output – current characteristics of samples. The threshold current of the samples was in the range from 250 to 270 mA, and the output cw power was of about 2 W for the pump current equal to 2.5 A.

Fig. 5 displays far-field patterns in the horizontal direction for sample No. 1 (the threshold current was of about

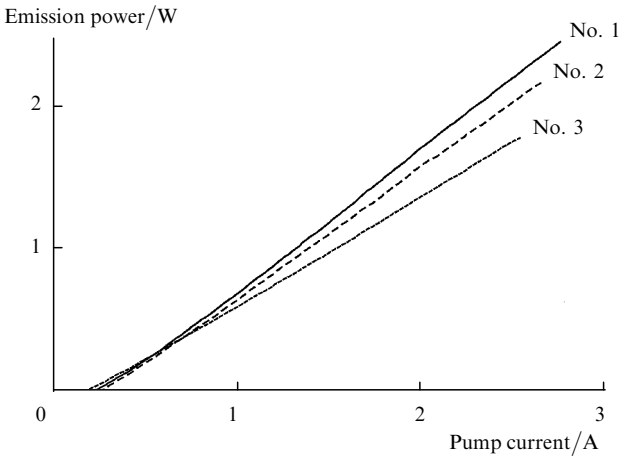

Figure 4. Light output – currentcharacteristics of samples Nos 1 – 3 for cw lasing.

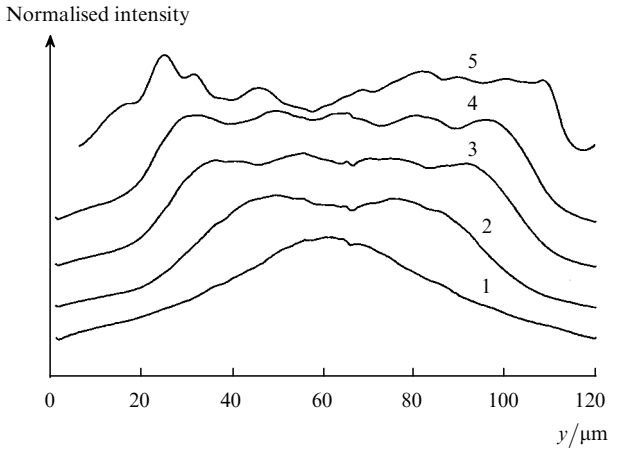

Figure 6. Intensities of the near-field pattern normalised to the maximum for sample No. 1 in the horizontal direction for pump currents 257 (1), 265 (2), 282 (3), 311 (4), and 1000 (5).

250 mA). Such radiation patterns are typical for these samples. Typical near-field patterns for the same sample (Fig. 6) demonstrate variations in the radiation intensity distribution along the exit laser mirror of length 100 μm with increasing current. One can see from far- and near-field patterns that lasing starts at the fundamental mode, which is favoured by the nearly diffraction divergence and the bell-shaped near-field intensity distribution (curves *1*, Figs 5 and 6).

However, for a current above 280 mA, the transverse distribution of the optical flux in the waveguide is somewhat distorted, which can be treated, in principle, as excitation of the higher horizontal modes. This is manifested in the broadening of the radiation pattern and in the variation of the near field. Note that the deformation of the optical flux at the laser exit mirror exhibits a typical quasi-periodic modulation of the transverse intensity distribution produced by the superposition of several horizontal modes. In this case, characteristic lobes appear in the far field at angles of about 1.5°, which correspond to the period of this structure. This is distinctly observed for currents up to 700 mA.

Such behaviour of the near-field pattern cannot be explained by conventional excitation of several transverse

modes. Indeed, the superposition of several independent transverse modes produces, as a rule, a complicated and irregular intensity distribution. In our case, the quasi-periodic distribution of the optical flux intensity was observed at the laser exit mirror for currents up to 320 mA.

An analysis in terms of the superposition of transverse modes is efficient when the transverse structure of an individual mode is retained and optical nonlinearity determines only the ratio of mode amplitudes. In the regime of the developed optical nonlinearity, as in our case, each individual mode undergoes self-deformation. Such a mode is called a nonlinear mode. In this case, the resulting transverse distribution of the field amplitudes cannot be treated as a superposition of transverse modes of a 'linear' (below the filamentation threshold) resonator. Formally, such a distribution can be considered as an expansion over any complete set of waves.

In our case, such a set can be formed by spatial harmonics in the yz plane (Fig. 1), i.e., plane waves. Then, the fundamental wave represents a fundamental spatially uniform wave, and the filamentation can be treated as excitation of the perturbation waves with a certain value of the transverse component of the wave vector or with a certain modulation period of the transverse intensity distribution.

One can see from Fig. 6 that the filament period decreases from approximately 50 μm (two maxima, curve *2*) to 20 μm (five maxima, curve *4*) with increasing intensity. The data presented and those obtained for other samples show that the modulation period quite sharply decreases with increasing intensity. Therefore, the regular intensity modulation on the laser mirror can be observed in most cases only near the lasing threshold. Thus, curve *4* in Fig. 6, which exhibits a distinct filamentation, corresponds only to the 20-% excess of the lasing threshold.

A further increase in the current and, respectively, in the radiation intensity results in excitation of a complete set of the perturbation waves with different transverse components of the wave vector. As a result, the intensity distribution corresponding to a power of about 1 W (curve *5*, Fig. 6) exhibits random behaviour both in the near and far fields. A specific near-field pattern under these conditions depends on the laser sample, which is obviously explained by the instability nature itself. Its manifestation is very sensitive to various optical properties of a specific laser.

However, a general property of the instability for all the samples investigated is, first, a low threshold for its appearance, which exceeds the lasing threshold no more than by 20%, and, second, characteristic values of the transverse wave vectors of the perturbation waves, which are excited first, i.e., the waves that exhibit the largest instability increment during the instability development. According to estimates based on the data presented in Fig. 5 (curves *2* and *3*) and Fig. 6 (curves *2–4*), the spatial period of harmonics is 10 – 50 μm, which is of the same order of magnitude as the values obtained in Refs [4, 5].

The dependences of the radiation brightness on the pump current for samples Nos 1 – 3 are shown in Fig. 7. Due to the filamentation development, the brightness changes in a complicated way. As a result, the brightness increases weakly compared to an 'ideal' case shown by the dashed straight line calculated in the absence of filamentation. The nonmonotonic dependence of the brightness on the current is caused by the random redistribution of the radiation intensity in the far zone of laser radiation, which affects the value of $I_{\max}(\varphi)$ in Eqn (5). One can see from Fig. 7 that the brightness of the samples studied also varies irregularly with the current. This suggests that the filamentation behaviour weakly depends on the waveguide design. The maximum radiation brightness is $\sim 1.7 \times 10^7$ W cm^{-2} sr^{-1}. It is achieved for the pump current of 2.5 A, which corresponds to the total output power ~ 2 W (Fig. 3).

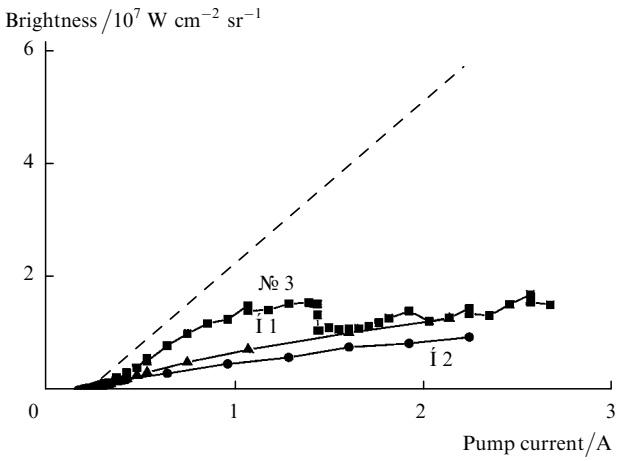

Figure 7. Dependences of brightness of samples Nos 1 – 3 on the pump currents: The dashed straight line corresponds to the brightness in the absence of filamentation.

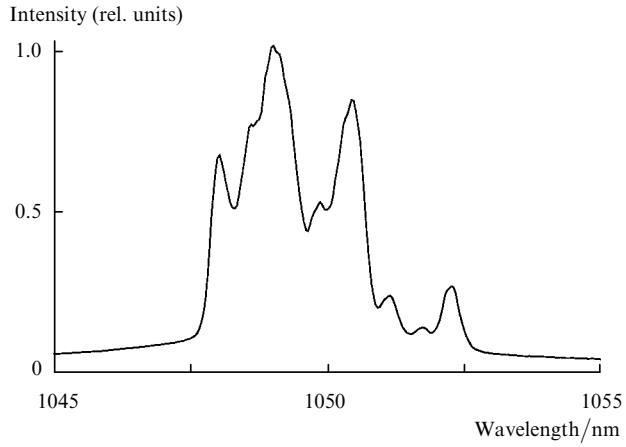

Figure 8. Emission spectrum of sample No. 1 for current 1.5 A.

The emission spectrum of lasers studied contained many longitudinal modes and its width was, as a rule, above 5 nm. Fig. 8 shows the spectrum of sample No. 1 for the current 1.5 A. For such an injection level, a great number of modes with different longitudinal and transverse indices are excited; the perturbation waves belong to the latter. These densely spaced modes are not resolved by a spectrometer (with a resolution of ~ 1 nm) and look like a continuous spectrum.

4. Conclusions

In this paper, we measured for the first time the radiation brightness for InGaAs/GaAs lasers with a broad active region. The maximum brightness was 1.7×10^7 W cm^{-2} sr^{-1} for the output power of 2 W. It was shown that filamentation appeared in quantum-well lasers studied when the pump current exceeded the lasing threshold by 10 – 20%, which corresponds to the optical power density equal to $\sim 3 \times 10^5$ W cm^{-2}. These values are close to those typical for

filamentation in AlGaAs heterojunction lasers. This conclusion indirectly confirms the results obtained in Ref. [10], according to which the factor α is between 2 and 9 for structures with analogous active media, which corresponds to a low filamentation threshold found in this paper.

We found that the filamentation period decreases with increasing output power from 50 μm immediately above the lasing threshold to $\sim$ 10 μm in the regime of the developed filamentation at large currents. This means that, in order to suppress the filamentation in lasers of this design using, for example, the α-DFB structure [9], it is necessary to use the parameters of the lattice that provide the efficient suppression of spatial harmonics of the perturbation waves with a period of about 10 μm and above.

According to previous papers [1 – 5], we can state that the brightness of the output radiation flux in samples studied is limited, first of all, by filamentation. The brightness that can be achieved is, as a rule, approximately lower by a factor of ten than its calculated value, which could be expected in the absence of filamentation. Therefore, the possibility exists for a strong enhancement of the radiation brightness of lasers of this type.

Acknowledgements. This work was supported by the Inter-industry Scientific and Technical Program 'Physics of Solid Nanostructures' and partially supported by the 'Integration' program, and by projects of the Educational Scientific Centre 'Fundamental Optoelectronics of Quantum-Well Semi-conductor Structures' and 'Fundamental Optics and Spectroscopy'.

References

1. Bakhert Kh-Yu, Bogatov A P, Eliseev P G Kvantovaya Elektron. (Moscow) **5** 603 (1978) [Quantum Electron. **8** 346 (1978)]
2. Tamburrini M, Goldberg L, Mehus D Appl. Phys. Lett. **60** 1292 (1992)
3. Paxton A H, Dente G C J. Appl. Phys. **70** 2921 (1991)
4. Bogatov A P Proc. SPIE-Int. Soc. Opt. Eng. **2399** 456 (1995)
5. Lang R J, Mehuys D, Welch D F, Goldberg L IEEE J. Quantum Electron. **30** 685 (1994)
6. Bespalov V I, Talanov V I Pis'ma Zh. Eksp. Teor. Fiz. **3** 471 (1966) [Sov. Phys. ZETP Lett. (1966)]
7. Parke R, Welch D F, Hardy A, Lang R, Mehuys D, O'Brien S, Dzurko K, Scrifres D IEEE Phot. Technol. Lett. **5** 297 (1993)
8. Guel-Sandoval S, et al. Appl. Phys. Lett. **66** 2048 (1995)
9. Dzurko K M, Lang R J, Scfres D R, Hardy A Proc. LEOS'95 (San Fransisco, 1995), vol. 2, p. 400
10. Bogatov A P, Boltaseva A E, Drakin A E, Belkin M A, Konyaev V P Kvantovaya Elektron. (Moscow) **30** 315 (2000) [Quantum Electron. **30** 315 (2000)]